ACADEMIC PRESS

Available online at www.sciencedirect.com

SCIENCE DIRECT®

Journal of Sound and Vibration 261 (2003) 895–910

JOURNAL OF SOUND AND VIBRATION

www.elsevier.com/locate/jsvi

Shape design sensitivity analysis for the radiated noise from the thin-body

Jeawon Lee, Semyung Wang*

Department of Mechatronics, Kwangju Institute of Science and Technology, 1 Oryong-dong, Puk-gu, Kwangju 500-712, South Korea

Received 11 December 2001; accepted 6 June 2002

Abstract

Many industrial applications generally use thin-body structures in their design. To calculate the radiated noise from vibrated structure including thin bodies, the conventional boundary element method (BEM) using the Helmholtz integral equation is not an effective resolution. Thus, many researchers have studied to resolve the thin-body problem in various physical fields. No major study in the design sensitivity analysis (DSA) fields for thin-body acoustics, however, has been reported.

A continuum-based shape DSA method is presented for the radiated noise from the thin-body. The normal derivative integral equation is employed as an analysis formulation. And, for the acoustic shape design sensitivity formulation, the equation is differentiated directly by using material derivative concept. To solve the normal derivative integral equation, the normal velocities on the surface should be calculated. In the acoustic shape sensitivity formulation, not only the normal velocities on the surface are required but also derivative coefficients of the normal velocities (structural shape design sensitivity) are also required as the input. Hence, the shape design sensitivity of structural velocities on the surface, with respect to the shape change, should be calculated. In this research, the structural shape design sensitivities are also obtained by using a continuum approach. And both a modified interpolation function and the Cauchy principle value are used to regularize the singularities generated from the acoustic shape design sensitivity formulation.

A simple annular disk is considered as a numerical example to validate the accuracy and efficiency of the shape design sensitivity equations derived in this research. The commercial BEM code, SYSNOISE, is utilized to confirm the results of the developed in-house code based on a normal derivative integral equation. To validate the calculated design sensitivity results, central finite difference method (FDM) is employed. The error between FDM and the analytical result are less than 3%. This comparison demonstrates that the proposed design sensitivities of the radiated pressure are very accurate.

*Corresponding author. Tel.: +82-62-970-2390; fax: +82-62-970-2384.
E-mail address: smwang@kjist.ac.kr (S. Wang).

0022-460X/03/$ - see front matter
PII: S0022-460X(02)01019-2

1. Introduction

Thin-body structures are frequently used for the design of many industrial applications such as fins or opened shells. To solve the acoustic problem including thin bodies, the conventional boundary element method (BEM) using the Helmholtz integral equation is not an effective resolution because the mesh on one side of a thin-body is too close to the mesh on the opposite side. Although that difficulty can be overcome by using very fine meshes, the process requires too much preprocessing and calculation time. Moreover, the nearly singular problem may occur in the integral equation. Thus, many researchers have tried to solve the thin-body problem in various physical fields including acoustics, electromagnetics and solid mechanics.

The multi-domain BEM [1] is the simplest way to handle the thin-body problem theoretically. Even though the concept of multi-domain BEM is simple and straightforward, it is not very efficient in computation when the imaginary interface surface is relatively large. In the normal derivative integral equation, proposed by Wu and Wan [2], an imaginary interface surface is also constructed like the multi-domain BEM. Furthermore, the Helmholtz integral equations and the normal derivative integral equations are constructed for each subdomain including both a structural surface and an imaginary surface. The integrals over the imaginary interface surface, however, are simply canceled out due to continuity of pressure and velocity after combining the Helmholtz integral equations with its normal derivative equation. Therefore, only the neutral surface of the thin-body remains for the discretization. The normal derivative integral equation approach, however, involves the evaluation of a hyper-singular integral in order of $1/r^3$. So the regularization method, originally derived by Maue [3] and later by Mitzner [4], is utilized. The evaluation of the hyper-singular integral can be also avoided by adopting a variational formulation, proposed by Pierce et al. [5] The resulting coefficient matrix obtained from the variational formulation is symmetric, but the computational cost is relatively high because a double surface integral must be evaluated.

In the area of the design sensitivity analysis (DSA) for acoustics, not many studies have been reported by using the BEM. Kane et al. [6] presented a shape design sensitivity formulation method by using the implicit differentiation of the discretized Helmholtz integral equation. Koopmann et al. [7] studied the sensitivity of radiated acoustic power to the change of acoustic velocity for a given geometric configuration. Vlahopoulos [8] and Coytte et al. [9] also studied the sizing DSA of acoustic radiation problems. Smith and Bernhard [10] computed the sensitivity by differentiating the discretized boundary integral equation. The derivative of the system matrix was approximated by adopting the finite difference concept. Cunefare et al. [11,12] presented sizing acoustic DSA through chain-ruled derivatives from FEM and BEM codes. Their research had focused on the best optimization formulation by comparing the relative performance and results obtained through the use of several different objective functions and constraints. Bonnet [13,14] derived continuum differentiation of the conventional boundary integral equation. Wang and Lee [15] presented a sizing acoustic DSA method using a continuum approach.

In this research, a continuum-based shape DSA method is presented for the radiated noise from a thin-body. The normal derivative integral formulation is differentiated directly by using material derivative concept to get the acoustic shape design sensitivity. And the shape design sensitivities of structural velocities on the surface are also calculated with the continuum approach. As a

numerical example, a simple disk is considered to validate the accuracy and efficiency of derived shape design sensitivity equations in this research.

2. Acoustic shape design sensitivity formulation

2.1. Normal derivative integral equation

When a thin-body structure is vibrated with normal velocities $\mathbf{v}_n$, the radiated acoustic pressure at a field point $\hat{x}$ should be calculated by the normal derivative integral equation, proposed by Wu and Wan [2], i.e.,

$$\int_S \frac{\partial G(\hat{x},\hat{y})}{\partial \mathbf{n}} \mu \, \mathrm{d}S = \int_S (\nabla G \cdot \mathbf{n}) \mu \, \mathrm{d}S = p(\hat{x}). \tag{1}$$

In Eq. (1), $G(\hat{x},\hat{y})$ is the Green function, which is the function of distance R between the points $\hat{x}$ and $\hat{y}$. Point $\hat{x}$ is a field point located out of the surface and point $\hat{y}$ is on the surface. Hence, the integral in Eq. (1) should be calculated over the surface $S(\hat{y})$ with a fixed field point $\hat{x}$. And $\mathbf{n}$ is the normal vector of the surface, μ is the difference between outside and inside pressure on the surface and is called the jump of pressure or the double layer potential, $\mu \equiv p^+ - p^-$.

When the field point $\hat{x}$ is located on the surface, the normal derivative formulation is obtained as [2]

$$\int_S \{(\mathbf{n}_{\hat{x}} \times \nabla_{\hat{x}} G) \cdot (\mathbf{n} \times \nabla \mu) + k^2 (\mathbf{n}_{\hat{x}} \cdot \mathbf{n}) G \mu\} \, \mathrm{d}S = \frac{\partial p(\hat{x})}{\partial \mathbf{n}_{\hat{x}}} = -\mathrm{j}\omega\rho \mathbf{v}_n(\hat{x}). \tag{2}$$

In Eq. (2), $\mathbf{n}_{\hat{x}}$ is the normal vector at the point $\hat{x}$, the operator ∇ and $\nabla_{\hat{x}}$ denote the gradient with respect to the point $\hat{y}$ and $\hat{x}$, respectively. Although the Green function is symmetric, $G(\hat{x},\hat{y}) = G(\hat{y},\hat{x})$, its gradients are opposite due to the derivative point, $\nabla G = -\nabla_{\hat{x}} G$, because the derivative of distance R with respect to the point $\hat{y}$ is opposite to the derivative of the distance with respect to the point $\hat{x}$.

The radiated pressure $p(\hat{x})$ can be calculated from Eq. (1) with the value of double layer potential μ, which can be obtained from Eq. (2) with the known normal velocities $\mathbf{v}_n$ on the surface S. The numerical solution of Eqs. (1) and (2) can be obtained by discretizing the surface S of the thin-body structure into a number of elements. Using interpolating shape function, Eq. (1) can be discretized and rewritten in a matrix form

$$\mathbf{p}(\hat{x}) = \mathbf{M}_e \boldsymbol{\mu}, \tag{3}$$

where $\mathbf{p}(\hat{x})$ is the pressure at field points, $\boldsymbol{\mu}$ is a column vector composed by the values of double layer potential on the discretized surface, and $\mathbf{M}_e$ is the contribution matrix. If only one field point is considered, the contribution matrix should be a row vector. To solve Eq. (1) or Eq. (3), μ should be calculated from Eq. (4), which is the discretized equation in a matrix form of Eq. (2)

$$-\mathrm{j}\omega\rho \mathbf{v}_n = \mathbf{M}\boldsymbol{\mu}, \tag{4}$$

where $\mathbf{M}$ and $\mathbf{v}_n$ are the system matrix and the normal velocity vector, respectively.

2.2. Material derivative for shape sensitivity

For the shape DSA, the shape of the domain is treated as the design variable. When a domain Ω in one, two, or three dimensions, is changed with only one parameter τ, the transformation mapping is given by [16]

$$\begin{aligned} \hat{x}_\tau &\equiv T(\hat{x}, \tau), \\ \Omega_\tau &\equiv T(\Omega, \tau), \\ \Gamma_\tau &\equiv T(\Gamma, \tau). \end{aligned} \tag{5}$$

In Eq. (5), $\hat{x}$ and $\hat{x}_\tau$ denote the points in the domain Ω and Ω_τ, respectively. According to the mapping, the initial point $\hat{x}$ moves to $\hat{x}_\tau$. The process of deforming from Ω to Ω_τ by the mapping of Eq. (5) may be viewed as a dynamic process of deforming a continuum with τ playing the role of time. Thinking of τ as time, a design velocity field V can be defined as

$$V(\hat{x}_\tau, \tau) \equiv \frac{\mathrm{d}\hat{x}_\tau}{\mathrm{d}\tau} = \frac{\mathrm{d}T(\hat{x}, \tau)}{\mathrm{d}\tau} = \frac{\partial T(\hat{x}, \tau)}{\partial \tau}. \tag{6}$$

Design velocity field defined in Eq. (6) means the movement of the point in the domain with respect to the time change. In the neighborhood of initial time $\tau = 0$, assuming a certain regularity hypothesis and ignoring higher order terms, T can be approximated by

$$\begin{aligned} T(\hat{x}, \tau) &= T(\hat{x}, 0) + \tau \frac{\partial T(x, 0)}{\partial \tau} + O(\tau^2) \\ &= \hat{x} + \tau V(\hat{x}, 0) + O(\tau^2) \\ &\approx \hat{x} + \tau V(\hat{x}, 0) \\ &= \hat{x} + \tau V(\hat{x}). \end{aligned} \tag{7}$$

Consider an arbitrary function f defined in the domain Ω. As Fig. 1 indicates, according to the time τ, a point $\hat{x}$ and a function f should be changed to $\hat{x}_\tau$ and f_τ, respectively. The pointwise

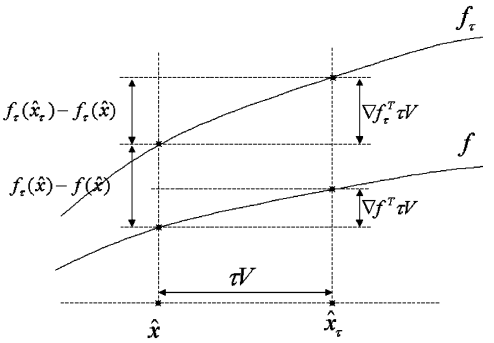

Fig. 1. Material derivative for a function f.

material derivative of the function f, if it exists, is defined as

$$\begin{aligned}\dot{f}(\hat{x}) &\equiv \frac{\mathrm{d}}{\mathrm{d}\tau} f_\tau(\hat{x}+\tau V(\hat{x}))\bigg|_{\tau=0} \\ &= \lim_{\tau\to 0}\frac{f_\tau(\hat{x}+\tau V(\hat{x}))-f(\hat{x})}{\tau} \\ &= \lim_{\tau\to 0}\frac{(f_\tau(\hat{x}_\tau)-f_\tau(\hat{x}))+(f_\tau(\hat{x})-f(\hat{x}))}{\tau} \\ &= \lim_{\tau\to 0}\frac{\nabla f_\tau^{\mathrm{T}}\tau V+(f_\tau(\hat{x})-f(\hat{x}))}{\tau}. \end{aligned} \tag{8}$$

If f_τ has a regular extension to a neighborhood of the closed set Ω_τ, then $\nabla f_\tau^{\mathrm{T}}\tau V(\hat{x})\cong\nabla f^{\mathrm{T}}\tau V(\hat{x})$ because of very small τ and Eq. (8) is rewritten as Eq. (9) with definition of Eq. (10)

$$\dot{f}(\hat{x}) = f'(\hat{x}) + \nabla f^{\mathrm{T}} V(\hat{x}), \tag{9}$$

$$f'(\hat{x}) \equiv \frac{\partial}{\partial\tau} f_\tau(\hat{x})\bigg|_{\tau=0} = \lim_{\tau\to 0}\frac{f_\tau(\hat{x})-f(\hat{x})}{\tau}. \tag{10}$$

∇f means a gradient vector, which is a derivative in the three co-ordinate directions. Both $\dot{f}$ and f' are the kinds of slopes for the function variation. By the definition of Eqs. (8)–(10), the pointwise material derivative $\dot{f}$ is a slope of function change from $f_\tau(\hat{x}_\tau)$ to $f(\hat{x})$ owing to the time change. And f' denotes the partial derivative of function f at the same point $\hat{x}$, it means a slope of function change from $f_\tau(\hat{x})$ to $f(\hat{x})$.

2.3. Acoustic shape design sensitivity formulation

Let a general functional ψ be defined as an integral over surface S with the direction vectors shown in Fig. 2

$$\Psi = \int_{S_\tau} g_\tau(\hat{y}_\tau)\,\mathrm{d}S_\tau. \tag{11}$$

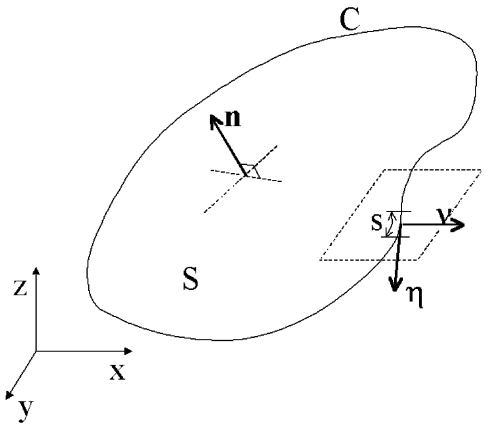

Fig. 2. Direction vectors for the surface (**n**—surface normal, η—boundary tangent, and ν—boundary normal).

The material derivative of ψ is [14,16]

$$\begin{aligned}\Psi' &= \int_S [\dot{g}(\hat{y}) + g(\hat{y})\mathrm{div}_s\,\mathbf{V}]\,\mathrm{d}S \\ &= \int_S [g'(\hat{y}) + (\nabla g(\hat{y})\cdot\mathbf{n} + Hg(\hat{y}))(\mathbf{V}\cdot\mathbf{n})]\,\mathrm{d}S + \int_C g(\hat{y})(\mathbf{V}\cdot\mathbf{v})\,\mathrm{d}s. \end{aligned} \tag{12}$$

In Eq. (12), $H \equiv \mathrm{div}\,\mathbf{n}$ and $\mathbf{V}$ is the design velocity field of the shape change. Physically, the material derivative ψ' means the change of the general functional ψ per unit change of the shape design variable. Since the final goal of this research is the shape DSA of the radiated pressure at a field point $\hat{x}$, the objective function of DSA is defined as

$$\Psi = p(\hat{x}) = \int_S (\nabla G\cdot\mathbf{n})\mu(\hat{y})\,\mathrm{d}S. \tag{13}$$

To get the material derivative of ψ or $p(\hat{x})$, treat $(\nabla G\cdot\mathbf{n})\mu$ as a general function g in Eq. (11). Then the partial derivative of g is

$$g' = [(\nabla G\cdot\mathbf{n})\mu]' = (\nabla G\cdot\mathbf{n})'\mu + (\nabla G\cdot\mathbf{n})\mu'. \tag{14}$$

Since the Green function and the normal vector are dependent on the geometry of the surface and its applied frequencies only, $(\nabla G\cdot\mathbf{n})'$ should be zero at same point. Accordingly, g' can be simplified as

$$g' = (\nabla G\cdot\mathbf{n})\mu'. \tag{15}$$

The ∇g can be derived as

$$\nabla g = \nabla(\nabla G\cdot\mathbf{n})\mu + (\nabla G\cdot\mathbf{n})\nabla\mu, \tag{16}$$

$$\begin{aligned}\nabla(\nabla G\cdot\mathbf{n}) &= (\mathbf{n}\cdot\nabla)\nabla G + (\nabla G\cdot\nabla)\mathbf{n} + \mathbf{n}\times(\nabla\times\nabla G) + \nabla G\times(\nabla\times\mathbf{n}) \\ &= \mathbf{n}\cdot\nabla(\nabla G) + \nabla G\cdot\nabla\mathbf{n} + \mathbf{n}\times(\nabla\times\nabla G) + \nabla G\times(\nabla\times\mathbf{n}). \end{aligned} \tag{17}$$

In Eq. (17), $\nabla\times\nabla G = 0$. Consequently, Eq. (16) can be rewritten as

$$\nabla g = [\mathbf{n}\cdot\mathbf{D}_{\nabla G} + \nabla G\cdot\mathbf{D}_{\mathbf{n}} + \nabla G\times\mathbf{R}]\mu + (\nabla G\cdot\mathbf{n})\nabla\mu. \tag{18}$$

In Eq. (18), $\mathbf{R}$ is the curl of normal vector $\mathbf{n}$ and $\mathbf{D}$ is the dyadic, which is a gradient of a vector. In this paper, $\mathbf{D}_{\mathbf{n}}$ is a gradient of the vector $\mathbf{n}$ and $\mathbf{D}_{\nabla G}$ is a gradient of the gradient of scalar function G. By substitution of Eqs. (15) and (18) into Eq. (12), the material derivative of Eq. (13) is derived as

$$\begin{aligned}\dot{p}(\hat{x}) = &\int_S \{(\nabla G\cdot\mathbf{n})\mu' + [(\mathbf{n}\cdot\mathbf{D}_{\nabla G} + \nabla G\cdot\mathbf{D}_{\mathbf{n}} + \nabla G\times\mathbf{R})\mu + (\nabla G\cdot\mathbf{n})\nabla\mu]\cdot n\}(V\cdot\mathbf{n})\,\mathrm{d}S \\ &+ \int_S \{[H(\nabla G\cdot\mathbf{n})(V\cdot\mathbf{n}) + (\nabla G\cdot\mathbf{n})\mathrm{div}\,V]\mu\}\,\mathrm{d}S. \end{aligned} \tag{19}$$

To get the shape design sensitivity of the pressure, $\dot{p}(\hat{x})$, the two variables μ' and μ must be known. The variable μ can be easily obtained from Eq. (2) with the known velocity on the surface $\mathbf{v}_n$. To obtain the variable μ', however, an additional equation is needed. If a general function f is defined as Eq. (20), then the material derivative of Eqs. (2) can be denoted as Eq. (21)

using Eq. (12)

$$f(\hat{y}) \equiv (\mathbf{n}_{\hat{x}} \times \nabla_{\hat{x}} G) \cdot (\mathbf{n} \times \nabla \mu(\hat{y})) + k^2 (\mathbf{n}_{\hat{x}} \cdot \mathbf{n}) G \mu(\hat{y}), \tag{20}$$

$$-\mathrm{j}\omega\rho \dot{\mathbf{v}}_n(\hat{x}) = \int_S [f'(\hat{y}) + (\nabla f(\hat{y}) \cdot \mathbf{n} + H f(\hat{y}))(\mathbf{V} \cdot \mathbf{n})] \, \mathrm{d}S + \int_C f(\hat{y})(\mathbf{V} \cdot \mathbf{v}) \, \mathrm{d}s. \tag{21}$$

Like the derivation of Eq. (19), f' and ∇f are needed for Eq. (21). The f' is

$$f' = (\mathbf{n}_{\hat{x}} \times \nabla_{\hat{x}} G) \cdot (\mathbf{n} \times \nabla \mu') + k^2 (\mathbf{n}_{\hat{x}} \cdot \mathbf{n}) G \mu'. \tag{22}$$

Using the symmetric condition of the Green function $\nabla G = -\nabla_{\hat{x}} G$,

$$f' = k^2 (\mathbf{n}_{\hat{x}} \cdot \mathbf{n}) G \mu' - (\mathbf{n}_{\hat{x}} \times \nabla G) \cdot (\mathbf{n} \times \nabla \mu'). \tag{23}$$

Since the Green function should satisfy the wave equation, $\nabla^2 G = k^2 G - \delta$. Using this relation, the ∇f is derived as

$$\begin{aligned}
\nabla f = {} & (\mathbf{n} \times \nabla \mu) \cdot \mathbf{D}_{\nabla G \times \mathbf{n}_{\hat{x}}} + (\nabla G \times \mathbf{n}_{\hat{x}}) \cdot \mathbf{D}_{\mathbf{n} \times \nabla \mu} \\
& + (\mathbf{n} \times \nabla \mu) \times [\nabla G H_{\hat{x}} - \nabla G \cdot \mathbf{D}_{\mathbf{n}_{\hat{x}}} + \mathbf{n}_{\hat{x}} \cdot \mathbf{D}_{\nabla G} + \mathbf{n}_{\hat{x}} (k^2 G - \delta)] \\
& + (\mathbf{n}_{\hat{x}} \times \nabla G) \times [\nabla \mu H - \nabla \mu \cdot \mathbf{D}_n + \mathbf{n} \cdot \mathbf{D}_{\nabla \mu} + \mathbf{n}(k^2 \mu)] \\
& + k^2 [\mathbf{n} \cdot \mathbf{D}_{\mathbf{n}_{\hat{x}}} + \mathbf{n}_{\hat{x}} \cdot \mathbf{D}_n + \mathbf{n} \times R_{\hat{x}} + \mathbf{n}_{\hat{x}} \times \mathbf{R}] G \mu \\
& + k^2 (\mathbf{n}_{\hat{x}} \cdot \mathbf{n}) \nabla G \mu + k^2 (\mathbf{n}_{\hat{x}} \cdot \mathbf{n}) G \nabla \mu.
\end{aligned} \tag{24}$$

In Eq. (24), $H_{\hat{x}}$ and $\mathbf{R}_{\hat{x}}$ denote the divergence and curl of the normal vector at the point $\hat{x}$, respectively. And the δ means the Dirac delta which has the value of one at the point $\hat{x}$ and zero for other points. Using Eqs. (23) and (24), Eq. (21) can be expanded as

$$\begin{aligned}
& -\mathrm{j}\omega\rho \dot{\mathbf{v}}_n(\hat{x}) \\
= {} & \int_S [k^2 (\mathbf{n}_{\hat{x}} \cdot \mathbf{n}) G \mu' - (\mathbf{n}_{\hat{x}} \times \nabla G) \cdot (\mathbf{n} \times \nabla \mu')] \, \mathrm{d}S \\
& + \int_S \{[(\mathbf{n} \times \nabla \mu) \cdot \mathbf{D}_{\nabla G \times \mathbf{n}_{\hat{x}}} + (\nabla G \times \mathbf{n}_{\hat{x}}) \cdot \mathbf{D}_{\mathbf{n} \times \nabla \mu}] \cdot \mathbf{n}\} (\mathbf{V} \cdot \mathbf{n}) \, \mathrm{d}S \\
& + \int_S \{[(\mathbf{n} \times \nabla \mu) \times (\nabla G H_{\hat{x}} - \nabla G \cdot \mathbf{D}_{\mathbf{n}_{\hat{x}}} + \mathbf{n}_{\hat{x}} \cdot \mathbf{D}_{\nabla G} + \mathbf{n}_{\hat{x}} (k^2 G - \delta))] \cdot \mathbf{n}\} (\mathbf{V} \cdot \mathbf{n}) \, \mathrm{d}S \\
& + \int_S \{[(\mathbf{n}_{\hat{x}} \times \nabla G) \times (\nabla \mu H - \nabla \mu \cdot \mathbf{D}_{\mathbf{n}} + \mathbf{n} \cdot \mathbf{D}_{\nabla \mu} + \mathbf{n}(k^2 \mu))] \cdot \mathbf{n}\} (\mathbf{V} \cdot \mathbf{n}) \, \mathrm{d}S \\
& + \int_S \{[k^2 (\mathbf{n} \cdot \mathbf{D}_{\mathbf{n}_{\hat{x}}} + \mathbf{n}_{\hat{x}} \cdot \mathbf{D}_{\mathbf{n}} + \mathbf{n} \times \mathbf{R}_{\hat{x}} + \mathbf{n}_{\hat{x}} \times \mathbf{R}) G \mu] \cdot \mathbf{n}\} (\mathbf{V} \cdot \mathbf{n}) \, \mathrm{d}S \\
& + \int_S \{[k^2 (\mathbf{n}_{\hat{x}} \cdot \mathbf{n}) \nabla G \mu + k^2 (\mathbf{n}_{\hat{x}} \cdot \mathbf{n}) G \nabla \mu] \cdot \mathbf{n}\} (\mathbf{V} \cdot \mathbf{n}) \, \mathrm{d}S \\
& + \int_S H [k^2 (\mathbf{n}_{\hat{x}} \cdot \mathbf{n}) G \mu - (\mathbf{n}_{\hat{x}} \times \nabla G) \cdot (\mathbf{n} \times \nabla \mu)] (\mathbf{V} \cdot \mathbf{n}) \, \mathrm{d}S \\
& + \int_S [k^2 (\mathbf{n}_{\hat{x}} \cdot \mathbf{n}) G \mu - (\mathbf{n}_{\hat{x}} \times \nabla G) \cdot (\mathbf{n} \times \nabla \mu)] (\mathrm{div} \mathbf{V}) \, \mathrm{d}S.
\end{aligned} \tag{25}$$

Since the single layer potential, which is the difference of the normal velocities on the outside and inside surface, $\sigma \equiv \mathbf{v}_n^+ - \mathbf{v}_n^-$, is zero for a thin-body problem, $\nabla\mu(\hat{x}) \cdot \mathbf{n}_{\hat{x}} = 0$. Therefore, the integration of the Dirac delta in Eq. (25) becomes zero.

$$
\begin{aligned}
&-\mathrm{j}\omega\rho\dot{\mathbf{v}}_n(\hat{x}) \\
&= \int_S [k^2(\mathbf{n}_{\hat{x}} \cdot \mathbf{n})G\mu' - (\mathbf{n}_{\hat{x}} \times \nabla G) \cdot (\mathbf{n} \times \nabla\mu')]\,\mathrm{d}S \\
&\quad + \int_S \{[(\mathbf{n} \times \nabla\mu) \cdot \mathbf{D}_{\nabla G \times \mathbf{n}_{\hat{x}}} + (\nabla G \times \mathbf{n}_{\hat{x}}) \cdot \mathbf{D}_{\mathbf{n} \times \nabla\mu}] \cdot \mathbf{n}\}(\mathbf{V} \cdot \mathbf{n})\,\mathrm{d}S \\
&\quad + \int_S \{[(\mathbf{n} \times \nabla\mu) \times (\nabla G H_{\hat{x}} - \nabla G \cdot \mathbf{D}_{\mathbf{n}_{\hat{x}}} + \mathbf{n}_{\hat{x}} \cdot \mathbf{D}_{\nabla G} + k^2 G\mathbf{n}_{\hat{x}})] \cdot \mathbf{n}\}(\mathbf{V} \cdot \mathbf{n})\,\mathrm{d}S \\
&\quad + \int_S \{[(\mathbf{n}_{\hat{x}} \times \nabla G) \times (\nabla\mu H - \nabla\mu \cdot \mathbf{D}_{\mathbf{n}} + \mathbf{n} \cdot \mathbf{D}_{\nabla\mu} + k^2\mu\mathbf{n})] \cdot \mathbf{n}\}(\mathbf{V} \cdot \mathbf{n})\,\mathrm{d}S \\
&\quad + \int_S \{[k^2(\mathbf{n} \cdot \mathbf{D}_{\mathbf{n}_{\hat{x}}} + \mathbf{n}_{\hat{x}} \cdot \mathbf{D}_{\mathbf{n}} + \mathbf{n} \times \mathbf{R}_{\hat{x}} + \mathbf{n}_{\hat{x}} \times \mathbf{R})G\mu] \cdot \mathbf{n}\}(\mathbf{V} \cdot \mathbf{n})\,\mathrm{d}S \\
&\quad + \int_S \{[k^2(\mathbf{n}_{\hat{x}} \cdot \mathbf{n})\nabla G\mu + k^2(\mathbf{n}_{\hat{x}} \cdot \mathbf{n})G\nabla\mu] \cdot \mathbf{n}\}(\mathbf{V} \cdot \mathbf{n})\,\mathrm{d}S \\
&\quad + \int_S H[k^2(\mathbf{n}_{\hat{x}} \cdot \mathbf{n})G\mu - (\mathbf{n}_{\hat{x}} \times \nabla G) \cdot (\mathbf{n} \times \nabla\mu)](\mathbf{V} \cdot \mathbf{n})\,\mathrm{d}S \\
&\quad + \int_S [k^2(\mathbf{n}_{\hat{x}} \cdot \mathbf{n})G\mu - (\mathbf{n}_{\hat{x}} \times \nabla G) \cdot (\mathbf{n} \times \nabla\mu)](\mathrm{div}\,\mathbf{V})\,\mathrm{d}S. \qquad (26)
\end{aligned}
$$

In Eq. (19), the field point $\hat{x}$ is located out of the surface and the point $\hat{y}$ is located on the surface. Therefore, the point $\hat{x}$ is not moving when the shape of the structure is changed. In Eq. (26), however, not only $\hat{y}$ but also $\hat{x}$ is located on the surface. So the point $\hat{x}$ is also moved when the shape is changed. It means that the design velocity field $\mathbf{V}$ has to be different for the Eqs. (19) and (26).

$$
\mathbf{V} = \begin{cases} \mathbf{V}(\hat{y}) & \text{for Eq. (19),} \\ \mathbf{V}(\hat{y}) - \mathbf{V}(\hat{x}) & \text{for Eq. (26).} \end{cases} \qquad (27)
$$

Eqs. (19) and (26) can be also discretized in matrix forms

$$
\dot{\mathbf{p}}(\hat{x}) = \mathbf{M}_e\boldsymbol{\mu}' + \mathbf{M}_e^D\boldsymbol{\mu}, \qquad (28)
$$

$$
-\mathrm{j}\omega\rho\dot{\mathbf{v}}_n = \mathbf{M}\boldsymbol{\mu}' + \mathbf{M}^D\boldsymbol{\mu}. \qquad (29)
$$

In Eqs. (28) and (29), $\mathbf{M}_e^D$ and $\mathbf{M}^D$ are material derivatives of the contribution and the system matrices, respectively. Since Eqs. (28) and (29) are discretized after differentiation, the solution of those are more accurate than the sensitivity result of directly differentiated equation of discretized formulation. In Eq. (28), the unknown variable $\boldsymbol{\mu}$ can be obtained from Eq. (4) with the normal velocities of the structure, $\mathbf{v}_n$, and $\boldsymbol{\mu}'$ can be calculated from Eq. (29) with the sensitivities of normal vectors, $\dot{\mathbf{v}}_n$. The structural shape design sensitivity $\dot{\mathbf{v}}_n$ in Eq. (29) means the change of normal velocities per unit change of the shape design variable. Therefore, the shape design

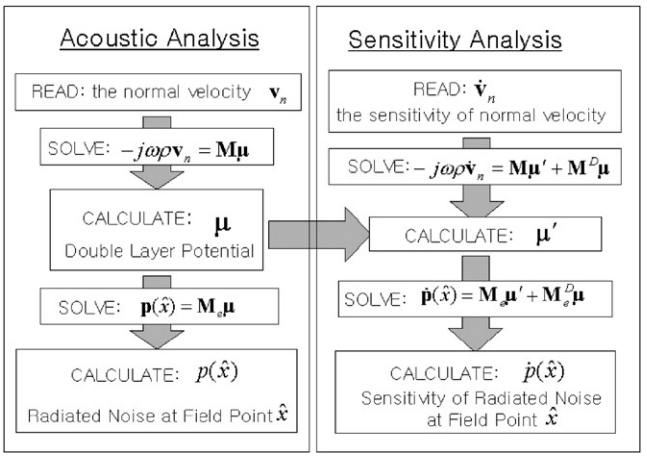

Fig. 3. Calculation procedures of acoustic analysis and sensitivity analyses.

sensitivity of the radiated noise at field points can be calculated by solving Eqs. (4), (28) and (29) with the normal velocity and its structural shape design sensitivities at each node point. These procedures are shown in Fig. 3.

When the point $\hat{x}$ and $\hat{y}$ are located on the same surface, the boundary integral equation has a singularity problem. There is no singularity problem in Eqs. (1) and (19) because the point $\hat{x}$ is located out of the surface. Since the field point $\hat{x}$ in Eq. (2) is located on the surface; however, Eq. (2) has a $O(1/r^2)$ singularity. The second order singularity can be solved by adopting the Cauchy principle value (CPV) idea. In Eq. (26), the sensitivity formulations of Eq. (2), the third order singularity is caused by a dyadic of the gradient of the Green function. Consequently, the other regularization is required. Fortunately, the dyadic in Eq. (26) must be multiplied by a design velocity field and the design velocity field in Eq. (26) is the difference of the values at points $\hat{x}$ and $\hat{y}$. Bonnet [14] proposed the modified interpolation function based on the introduction of polar coordinates in the parent element. By using the modified interpolation function, the third order singularity can be reduced to the second order. Accordingly, using CPV, the integrals of all acoustic equations derived in this research can be obtained.

3. Structural shape design sensitivity formulation

As shown in Fig. 3, sensitivity coefficients of the normal velocities on the surface are required as the input of acoustic shape design sensitivity formulation. The variational equation of a dynamic frequency response problem can be written for all $\bar{z} \in Z$ as

$$b_\Omega(z,\bar{z}) \equiv \int_\Omega f(z,\bar{z})\,\mathrm{d}\Omega = -\omega^2\rho d_\Omega(z,\bar{z}) + \mathrm{i}\omega c_\Omega(z,\bar{z}) + a_\Omega(z,\bar{z}) = l_\Omega(\bar{z}). \tag{30}$$

In Eq. (30), $a_\Omega(z,\bar{z})$ is the strain energy bilinear form, $c_\Omega(z,\bar{z})$ is the bilinear form due to the damping of the structure, $d_\Omega(z,\bar{z})$ is the mass effects bilinear form and $l_\Omega(\bar{z})$ is the load linear form.

The first variation of Eq. (30) is [16]

$$[b_\Omega(z,\bar{z})]' = b_\Omega(\dot{z},\bar{z}) + b_\Omega(z,\dot{\bar{z}}) - b_\Omega(\nabla z\cdot\mathbf{V},\bar{z}) - b_\Omega(z,\nabla\bar{z}\cdot\mathbf{V}) + b^0_\Omega(z,\bar{z})$$
$$= l'_V(\bar{z}) = [l_\Omega(\bar{z})]', \tag{31}$$

$$b^0_\Omega(z,\bar{z}) = \int\int_\Omega \mathrm{div}[f(z,\bar{z})\mathbf{V}_\Omega]\,\mathrm{d}\Omega, \tag{32}$$

where $f(z,\bar{z})$ is a bilinear mapping.

The differentials $b'_V(z,\bar{z})$ and $l'_V(\bar{z})$ in Eq. (31) denote the explicit dependence of energy and load forms due to the shape and orientation changes. In Eq. (31), $b'_V(z,\bar{z})$ is defined as

$$b'_V(z,\bar{z}) = -b_\Omega(\nabla z\cdot\mathbf{V},\bar{z}) - b_\Omega(z,\nabla\bar{z}\cdot\mathbf{V}) + b^0_\Omega(z,\bar{z}). \tag{33}$$

From Eq. (31) and using the fact that $\dot{\bar{z}}\in Z$ and $b_\Omega(z,\dot{\bar{z}}) = l_\Omega(\dot{\bar{z}})$, the first variation of Eq. (30) is

$$b_\Omega(\dot{z},\bar{z}) = l'_V(\bar{z}) - b'_V(z,\bar{z}) \quad \text{for all } \bar{z}\in Z. \tag{34}$$

Next, consider a general functional that may be written in domain integral form as

$$\Psi'_\tau = \int_{\Omega_t} g(z_\tau,\nabla z_\tau)\,\mathrm{d}\Omega_\tau, \tag{35}$$

where $\nabla z = [\nabla z_1\nabla z_2\nabla z_3]^{\mathrm{T}}$, and the function g is continuously differentiable with respect to its arguments. The variation of the functional of Eq. (35) is [16]

$$\Psi' = \int_\Omega [g_z z' + g_{\nabla z}\nabla z' + (\nabla g\cdot\mathbf{V}) + g\,\mathrm{div}\mathbf{V}]\,\mathrm{d}\Omega, \tag{36}$$

where, g_z is a derivative of g with respect to z and $g_{\nabla z}$ is a derivative of g with respect to the gradient of z.

Eq. (36) is rewritten as

$$\Psi' = \int_\Omega [g_z\dot{z} + g_{\nabla z}\nabla\dot{z} - g_z(\nabla z\cdot\mathbf{V}) - g_{\nabla z}\nabla(\nabla z\cdot\mathbf{V}) + (\nabla g\cdot\mathbf{V}) + g\,\mathrm{div}\mathbf{V}]\,\mathrm{d}\Omega, \tag{37}$$

where $\dot{z} = z' + (\nabla z\cdot\mathbf{V})$ and $\nabla\dot{z} = \nabla z' + \nabla(\nabla z\cdot\mathbf{V})$.

The objective here is to obtain an explicit expression for Ψ' in terms of the velocity field, which requires rewriting the first two terms of Eq. (37) explicitly in terms of velocity, i.e., eliminating $\dot{z}$. To eliminate $\dot{z}$, an adjoint equation is introduced by replacing $\dot{z}\in Z$ in Eq. (37) by a virtual displacement $\bar{\lambda}\in Z$ and equating the sum of terms involving $\bar{\lambda}$ to the bilinear form

$$b_\Omega(\lambda,\bar{\lambda}) = \int_\Omega [g_z\bar{\lambda} + g_{\nabla z}\nabla\bar{\lambda}]\,\mathrm{d}\Omega \quad \text{for all } \bar{\lambda}\in Z. \tag{38}$$

Using an adjoint approach, Eq. (37) becomes

$$\Psi' = l'_V(\lambda) - b'_V(z,\lambda) - \int_\Omega [g_z(\nabla z\cdot\mathbf{V}) + g_{\nabla z}\nabla(\nabla z\cdot\mathbf{V}) + (\nabla g\cdot\mathbf{V}) + g\,\mathrm{div}\mathbf{V}]\,\mathrm{d}\Omega. \tag{39}$$

Therefore, the right-hand can be evaluated once the state z and the adjoint variable λ are determined as the solutions of Eqs. (30) and (38).

To calculate the structural shape design sensitivities $\dot{\mathbf{v}}_n$ in Eq. (29), first consider the structural displacement at a point $\hat{x}$ in the domain Ω by the structure under harmonic excitation as a general

functional

$$\Psi = \int_{\Omega} \delta(x - \hat{x}) z_i \, d\Omega, \quad i = 1, 2, 3. \tag{40}$$

Since Eq. (40) is a function of z, the design sensitivity expression of Eq. (39) can be rewritten as

$$\Psi' = l'_V(\lambda) - b'_V(z, \lambda) - \int_{\Omega} [g_z(\nabla z \cdot \mathbf{V}) + (\nabla g \cdot \mathbf{V}) + g \, \mathrm{div}\mathbf{V}] \, d\Omega. \tag{41}$$

And the adjoint equation, Eq. (38), can be obtained as

$$b_{\Omega}(\lambda, \bar{\lambda}) = \int_{\Omega} \frac{\partial}{\partial z}[\delta(x - \hat{x})]\bar{\lambda} \, d\Omega = \int_{\Omega} \delta(x - \hat{x})\bar{\lambda} \, d\Omega. \tag{42}$$

With the original displacement z obtained from Eq. (30) and adjoint displacement λ obtained from Eq. (42), the shape design sensitivity of structural displacement can be calculated from Eq. (41). The structural shape design sensitivities of the normal velocity $\dot{\mathbf{v}}_n$ in Eq. (29) can be obtained by multiplying a scale factor to the displacement sensitivity result.

4. Numerical example

A simple annular disk is considered as a numerical example to validate the accuracy of the shape design sensitivity formulations. As shown in Fig. 4, this example is motivated by the noise of hard disk drive. Its inner boundary circle is clamped with radius 'a' and outer boundary circle is considered as a free end with radius 'b'. The number of elements for its numerical model was decided on 96 after the element convergence test by using the structural modes, as shown in Table 1.

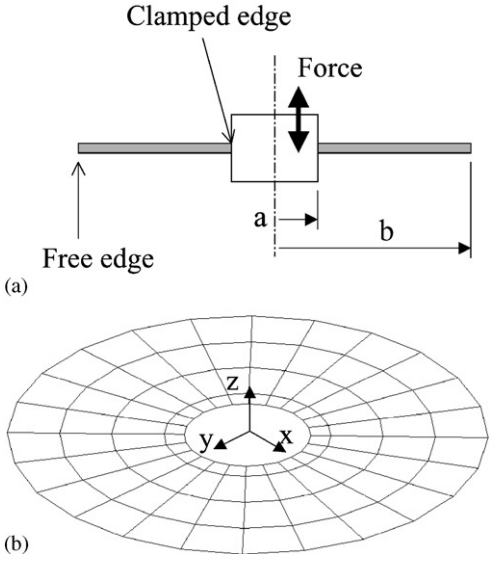

Fig. 4. Annular disk model: (a) schematic diagram and (b) FE and BE models.

Table 1
Element convergence test (Hz)

	Number of elements			Experiment
	48	96	144	
First mode (0,2)[a]	359.0	419.5	425.6	423.9
Second mode (0,0)	426.8	668.2	705.2	656.9
Third mode (0,3)	807.6	1010.6	1035.9	1056.9

[a] (m, n) = number of nodal circles, number of nodal diameters.

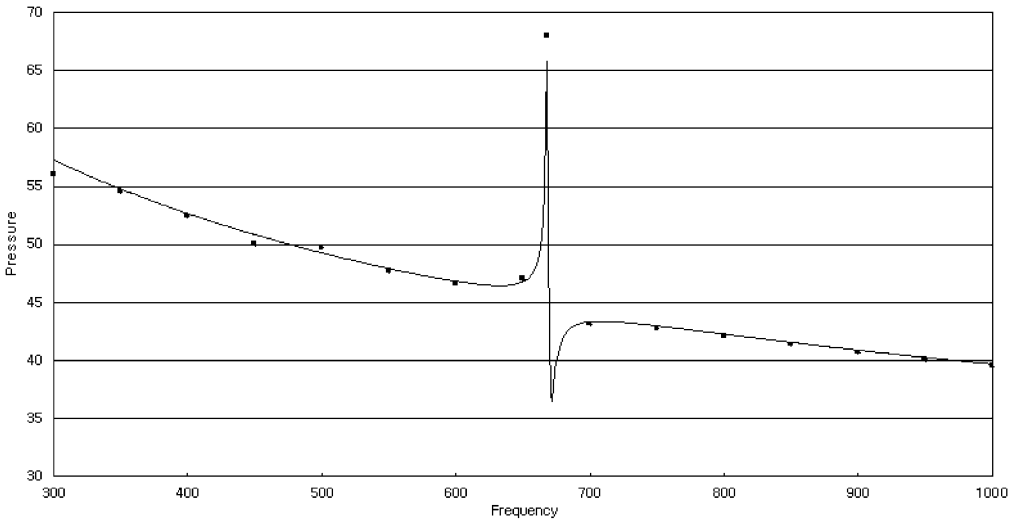

Fig. 5. Acoustic analysis results for the annular disk (—, indirect variational method by SYSNOISE; ■, normal derivative integral equation).

When the external forces are applied to the clamped edge, the structural normal velocities on the surface are calculated by MSC/NASTRAN. And using these normal velocities, the frequency responses of the acoustic pressure at $(0, 0, z)$ point, which is above the center of the thin-body disk, are calculated. The analysis results of the normal derivative integral equation are shown in Fig. 5. For the accurate sensitivity results, the analysis results should be accurate. In this paper, the commercial code SYSNOISE, which uses the indirect variational formulation for a thin-body, is used for the comparison of the results. As shown in Fig. 5, the analysis using normal derivative integral formulation is well matched with SYSNOISE. The analysis result shows the first peak is located at 668 Hz. It is the second mode of the structure in Table 1.

Since the goal of this research is not an optimization but a DSA, only the accuracy of the sensitivity coefficient is validated. For the sensitivity analysis, 668 Hz is decided as the target frequency and two shape design variables shown in Fig. 6 are selected. The positive directions of

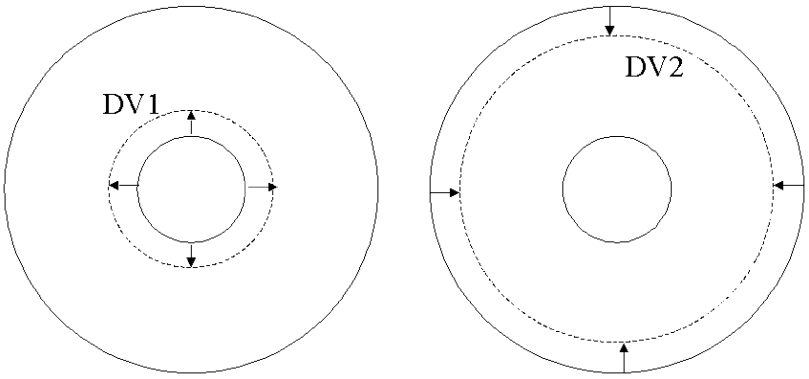

Fig. 6. Design variables of shape change (DV1 and DV2).

both design changes are set to reduce the surface area. For the shape DSA, three input variables are needed. First one is the normal velocity of the surface that is a result of the structural analysis. Moreover, the second one is the double layer potential that is calculated from Eq. (2) using the normal velocity. Fig. 7 shows the normal velocity and the double layer potential of the surface. Since the system is axisymmetric, only one side of disk section is plotted in Fig. 7. For the acoustic DSA, the structural sensitivity of the normal velocity must be calculated from the derived formulation in Section 3. This structural sensitivity results are shown in Fig. 8. The positive sensitivity means if the shape is changed along positive design variable direction, the performance should be increased. For instance, when the inner diameter of the disk is increased, the velocity at the inner circle should be increased and the velocity at the outer circle should be decreased. As shown in Fig. 8, the sensitivity results of the two design variables have the opposite tendency for each other.

Finally, the shape design sensitivity of the acoustic pressure at a field point is calculated. To verify the calculated design sensitivity results, central finite difference method obtained by SYSNOISE is employed in Table 2. As shown in Table 2, the sensitivity result is positive for the design variable 1 and negative for the design variable 2. Moreover, their magnitudes differ greatly from the order. In general, the acoustic pressure generated from the structural vibration is proportional to the product of velocity and surface area. For the design variable 1, although the positive part looks bigger than the negative part in Fig. 8, the integration of the changed velocities over the surface has a minus value because the inner part of the circular disk has smaller area than outer part. The final acoustic design sensitivity, however, is positive. It means that the sensitivity of the pressure is greatly influenced by the distance between an observing point and the source point for this example at least. When the design variable 1 is changed positively, the velocities of the surface near the observing point are increased and the pressure at the observing point is increased even though some velocities on the far points are decreased. For the design variable 2, the opposite results occur. Furthermore, the difference between the magnitudes of the structural sensitivities is also amplified by the effect of acoustic calculation. Table 2 also shows the design sensitivities of the radiated pressure with respect to both design variables 1 and 2 are very accurate.

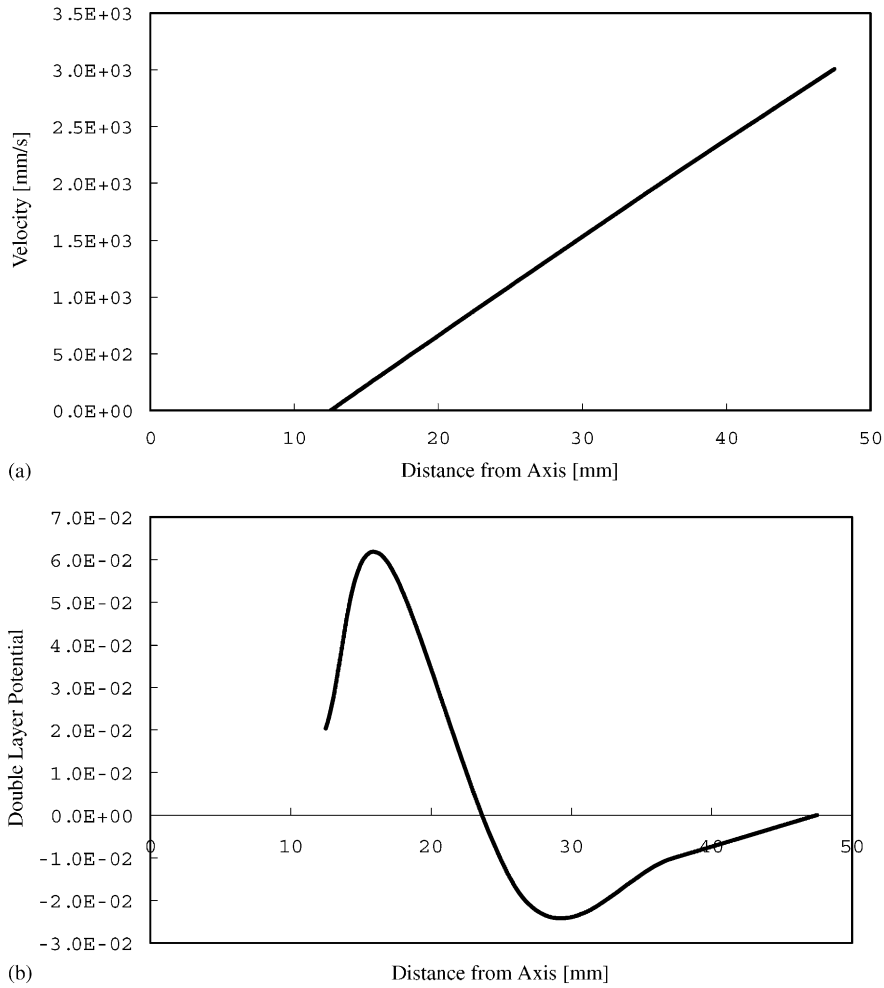

Fig. 7. Results of the structural and acoustic analysis: (a) structural velocity of the disk at 668 Hz and (b) double layer potential on the disk at 668 Hz.

5. Conclusion

The design sensitivity formulations of the radiated noise from thin-body with respect to the shape change are successfully derived and implemented. Using a simple model, the annular disk, the accuracy of calculated sensitivity results are validated. Nevertheless, there is a limitation of this approach. Derived equation works only to examples with the in-plane or orientation change of the smooth surface. Further research is required because the Cauchy principle value integral is distorted by a shape perturbation when the curvature of the surface is rapidly changed. Hence, the more general regularized method should be considered to reduce the order of singularity later on.

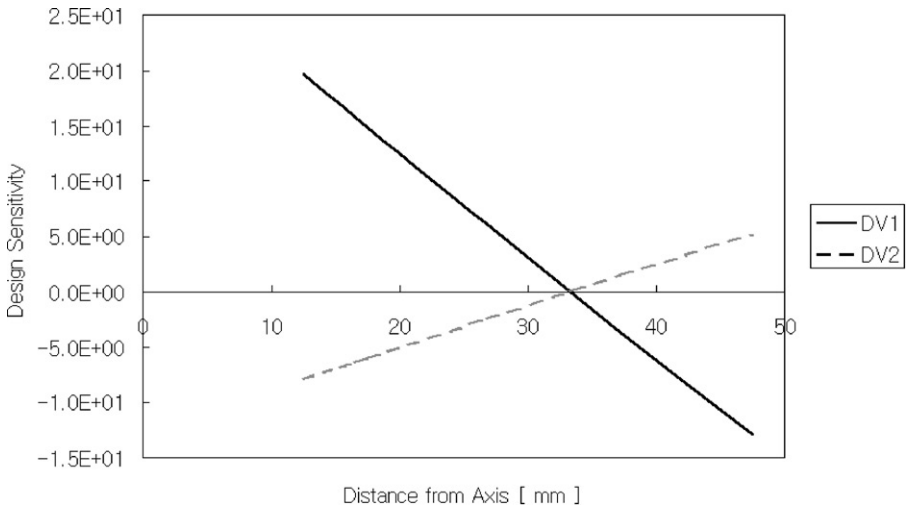

Fig. 8. Shape design sensitivity result of the normal velocity.

Table 2
Sensitivity verification for both DV1 and DV2

Design variable	Perturbation		$\Psi(d+\delta d)$ (Pa)	$\Psi(d+\delta d)$ (Pa)	$\Delta\Psi$[a]	Ψ'	Accuracy ($\Psi'/\Delta\Psi$) (%)
	(%)	(mm)					
DV1	0.1	0.0125	5.2123e−2	5.2102e−2	2.1e−4	2.047e−4	97.5
	0.01	0.00125	5.2111e−2	5.2109e−2	2.1e−4		**97.5**
DV2	0.1	0.0475	5.1874e−2	5.2316e−2	−1.768e−2	−1.858e−2	105.7
	0.01	0.00475	5.2092e−2	5.2137e−2	−1.800e−2		**103.2**

[a] $\Delta\Psi = \dfrac{\Psi(d+\delta d) - \Psi(d-\delta d)}{2\delta d}$, central finite difference and Ψ' is an analytical sensitivity result.

Acknowledgements

The Brain Korea 21 Project and the Center for Innovative Design Optimization Technology supported this research.

References

[1] A.F. Seybert, C.Y.R. Cheng, T.W. Wu, A multidomain boundary element solution for silencer and muffler performance prediction, Journal of Sound and Vibration 151 (1991) 119–129.
[2] T.W. Wu, G.C. Wan, Numerical modeling of acoustic radiation and scattering from thin bodies using a Cauchy principal integral equation, Journal of Acoustical Society of America 92 (1992) 2900–2906.
[3] A.W. Maue, Zur Formulierung eines allgemeinen Beugungsproblems durch eine Integralgleichung, Zeitschrift für Physik 126 (1949) 601–618.

[4] K.M. Mitzner, Acoustic scattering from an interface between media of greatly different density, Journal of Mathematical Physics 7 (1966) 2053–2060.
[5] X.F. Wu, A.D. Pierce, J.H. Ginsberg, Variational method for computing surface acoustic pressure on vibrating bodies, applied to transversely oscillating disks, IEEE Journal of the Oceanic Engineering OE-12 (1987) 412–418.
[6] J.H. Kane, S. Mao, G.C. Everstine, A boundary element formulation for acoustic shape sensitivity analysis, Journal of Acoustical Society of America 90 (1991) 561–573.
[7] R.R. Salagame, A.D. Belegundu, G.H. Koopmann, Acoustical sensitivity of acoustic power radiated from plate, Journal of Vibration and Acoustics 117 (1995) 43–48.
[8] N. Vlahopoulos, Boundary element formulation for acoustic sensitivities with respect to structural variables and acoustic impedance, Proceedings of the Second International Congress on Recent Developments in Air- and Structure-Borne Sound and Vibration, Auburn University, March 1992.
[9] J.P. Coytte, H. Wynendaele, M. Chargin, Evaluation of global acoustic sensitivities using a combined finite element/boundary element formulation, in: H.H. Hubbard (Ed.), Proceedings of Noise-Con 93(INCE/USA), Williamsburg, May 1993. Noise Control Foundation, Poughkeepsie, NY.
[10] D.C. Smith, R.J. Bernhard, Computation of acoustic shape design sensitivity using a boundary element method, Journal of Vibration and Acoustics 114 (1992) 127–132.
[11] S.P. Crane, K.A. Cunefare, S.P. Engelstad, E.A. Powell, Comparison of design optimization formulations for minimization of noise transmission in a cylinder, Journal of Aircraft 34 (1997) 236–243.
[12] K.A. Cunefare, S.P. Crane, S.P. Engelstad, E.A. Powell, Design minimization of noise in stiffened cylinders due to tonal external excitation, Journal of Aircraft 36 (1999) 563–570.
[13] M. Bonnet, M. Guiggiani, Tangential derivative of singular boundary integrals with respect to the position of collocation points, International Journal of Numerical Engineering 41 (1998) 1255–1275.
[14] M. Bonnet, Boundary Integral Equation Methods for Solids and Fluids, Wiley, Chichester, England, 1995.
[15] S. Wang, J. Lee, Acoustic design sensitivity analysis and optimization for reduced exterior noise, American Institute of Aeronautics and Astronautics Journal 39 (2001) 574–580.
[16] E.J. Haug, K.K. Choi, V. Komkov, Design Sensitivity Analysis of Structural System, Academic Press, New York, 1985.